Ab Initio Molecular Orbital Investigation of a Precursor in Ethylene Biosynthesis: Proton Transfer in a Cluster of 1-Aminocyclopropane-1-carboxylic Acid and Water

Mika Ito,[†] Suyong Re,[‡] and Hiroaki Tokiwa*[,†]

Department of Chemistry, Faculty of Science, Rikkyo University, 3-34-1 Nishi-ikebukuro, Toshima-ku, Tokyo 171-8501, Japan, and Department of Theoretical Studies, Institute for Molecular Science, 38 Myodaiji, Okazaki 444-8585, Japan

Received: October 9, 2003

The proton-transfer mechanism in hydrated 1-aminocyclopropane-1-carboxylic acid (ACC), which is a crucial precursor in the ethylene biosynthetic pathway in plants, was investigated by using an ab initio molecular orbital method to determine the importance of discrete water molecules in ethylene biosynthesis. Short-range local ACC−H_2O interactions are treated with the ACC·$(H_2O)_6$ cluster according to the analyses on the structures and stabilities of ACC·$(H_2O)_n$ ($n = 1-8$) clusters. Long-range solvent effects were taken into account by using the continuum model (Onsager model and polarizable continuum model (PCM)) of water. The combined approach of both discrete and continuum models showed that the zwitterionic form of the ACC·$(H_2O)_6$ cluster is 42.3 kJ mol^{-1} (ΔG) more stable than the neutral form at the level of B3LYP/6-31+G(d,p) with the PCM. The estimated energy barrier heights ($\Delta G^{\ddagger}$) for the neutral-to-zwitterion transition were 14.5 and 16.9 kJ mol^{-1} for the direct and water-assisted proton-transfer mechanisms. These results indicate the efficiency of both ionization mechanisms in water and suggest that water molecules interacting directly with ACC may have significant roles in the reaction that forms ethylene from ACC in aqueous solution.

1. Introduction

Ethylene, which is the simplest, smallest olefin, has received considerable attention during studies aimed at understanding several photochemical processes in biological systems. Detailed information has been obtained from both theoretical and experimental studies on the dynamics of ethylene transitions, such as its cis−trans isomerization.[1] In addition, this small molecule regulates many physiological processes in plant growth and development, as well established since its discovery by Neljubow.[2] Despite the apparent importance of ethylene as a plant hormone, the relevant mechanisms at the molecular level have been elusive.

It is now widely accepted that ethylene in higher plants can be produced from methionine through 1-aminocyclopropane-1-carboxylic acid (ACC) as a crucial intermediate (Scheme 1).[3−5] Once ACC was established as an immediate precursor of ethylene,[3] the enzymatic process converting ACC to ethylene has received much attention.[6] Many efforts have been paid to assay in vitro/in vivo the ethylene-forming enzyme (EFE) and to determine the genes encoding it.[7−13] Hamilton et al. discovered that the pTOM13 clone represents the gene encoding EFE and that the EFE catalyzes oxidation of ACC.[7,8] It has shown that this enzymatic reaction requires Fe(II), O_2, CO_2, and ascorbate.[9] The detail of chemical reaction mechanism of ethylene biosynthesis is still unclear, even though botanical study have suggested that *N*-hydroxyl-ACC is an intermediate, which would be then fragmented into ethylene and other species.[13] Despite the many experimental studies of ethylene, possible effects of the water molecules as the surrounding environment have never been explicitly treated. It is not surprising that water molecules can affect the above enzymatic reaction mechanism involving the electron and/or proton transfer. The nature of ACC precursor in water should be subjected to further studies to better understand ethylene biosynthesis in plants.

ACC has a similar backbone structure to glycine (Gly), which is the simplest amino acid and has thus been studied extensively. In particular, the exhaustive stability of the zwitterionic form of Gly, $^{+}NH_3-CH_2-COO^{-}$ (**Z**), in water over its neutral form, NH_2-CH_2-COOH (**N**) has been subjected to the number of theoretical studies.[14−23] In early theoretical studies, the effect of water was modeled by the continuum−solvation model[14−18] or by adding a few discrete water molecules.[19−23] Whereas Tomasi et al. concluded using the continuum model that the **Z** form was more stable than neutral Gly,[14] the continuum model may miss important contributions due to strong Gly−H_2O interactions. Jensen and Gordon showed with the discrete model that at least two water molecules are necessary to stabilize the glycine **Z**.[20] Recently, much effort has been made to simulate the effects of water more realistically by using a large-cluster model or hybrid quantum mechanical/molecular mechanical (QM/MM) methods.[24−29] Some of these calculations indicate that the neighboring water molecules have to be explicitly taken into account in order to correctly describe the **N**-to-**Z** transition of Gly in water.[24] In other words, neighboring water molecules play an important role not merely by affecting the microenvironment but as direct participants in determining the properties and reactions of Gly.

In this study, we investigated the **N**-to-**Z** transition of ACC as a first step in examining the significance of neighboring water molecules in ethylene biosynthesis. To fully take local ACC−water interactions into account, we analyzed the structure and stability of ACC·$(H_2O)_n$ ($n = 1-8$) clusters and looked for an adequate cluster model of solvated ACC. The adequate cluster model was embedded in a dielectric continuum. The combined

* To whom correspondence may be addressed. Phone/Fax: +81-3-3985-2394. E-mail: tokiwa@chem.rikkyo.ac.jp.
[†] Rikkyo University.
[‡] Institute for Molecular Science.

10.1021/jp031146y CCC: $27.50
Published on Web 05/29/2004

SCHEME 1. Ethylene Biosynthetic Pathway[10]

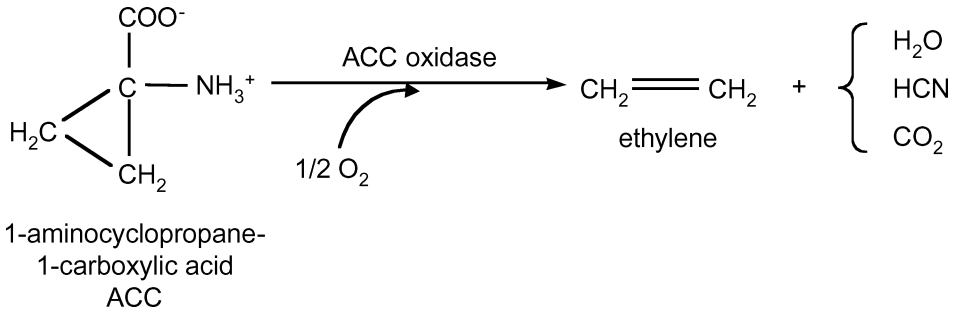

approach of applying both a discrete and a dielectric continuum model was used to explore whether the **N**-to-**Z** transition occurs via a water-assisted mechanism or not. The findings are of importance for eventually understanding whether ethylene in plants is created by an intramolecular process within ACC or by an intermolecular one involving ACC and water molecules.

2. Computational Methods

Density functional theory (DFT) methods are well established and have been used to investigate several types of phenomena in small molecules. In particular, systematic studies of hydrogen-bonded systems by the DFT method have verified that DFT can reasonably describe the thermodynamic characteristics of hydrogen bonding, as long as reliable basis sets are used.[30−40] We, therefore, used the B3LYP method, which is the Becke's three-parameter hybrid method using the LYP local and nonlocal exchange functionals of Lee, Yang, and Parr.[41,42] The Hatree−Fock calculations were also performed for comparison. In actual calculations, we adopted the 6-31G(d) basis set. To enable correct interpretation of the energy barrier heights for proton transfer, the 6-31+G(d,p) basis set was used for a certain calculation. The geometries of $ACC\cdot(H_2O)_n$ ($n = 1-8$) clusters were optimized by using the above methods. Long-range effects of solvent water medium were taken into account by means of a dielectric continuum represented by the Onsager model[43] and the polarizable continuum model (PCM).[44] For the $n = 6$ cluster, the optimization was performed with the dielectric continuum. Since the optimization using the PCM is hard to converge,[45] we used the Onsager model and the PCM for geometry optimizations and the energy refining, respectively. Each critical point was verified to be at an energy minimum by vibrational analysis based on the analytical second-derivative method. The continuum calculations were done with a dielectric constant $\epsilon = 78.5$ at 298.15 K and 0.1 MPa. All calculations were carried out with the Gaussian98 program package.[46]

3. Results and Discussion

3.1. Conformation of ACC. The three possible structures of the **N** form of ACC in the gas phase, as optimized at the B3LYP/6-31G(d) level, are shown in Figure 1a. The structure **N0c** has an intramolecular hydrogen bond (1.92 Å), while the structures **N0a** and **N0b** do not involve such a bond. In the gas phase, the former two structures are ∼2−3 kJ/mol less stable than the latter. This conformational preference is very similar

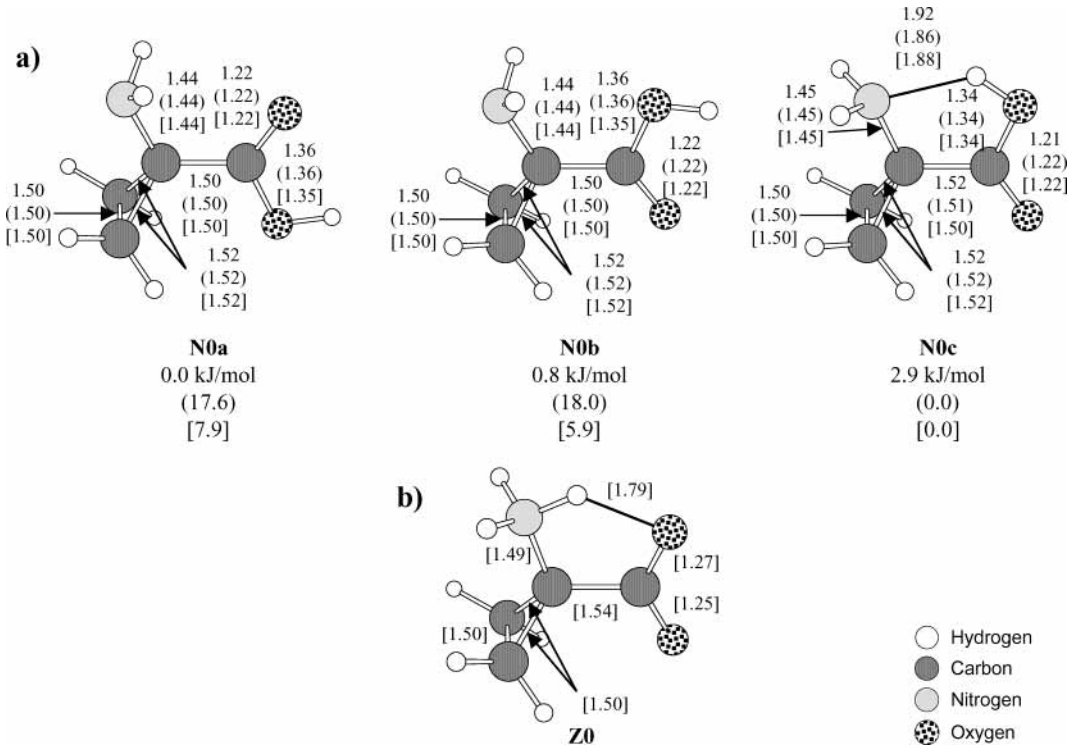

Figure 1. The **N** (a) and **Z** (b) structures of the ACC molecule in the gas phase and in the solution optimized at the B3LYP/6-31G(d) level. The geometry parameters from the top are the calculation of gas phase, solution using the Onsager model (in parentheses), and solution using the PCM model (in brackets), respectively. Bond lengths are shown in angstroms. The relative stabilities are shown in kJ/mol.

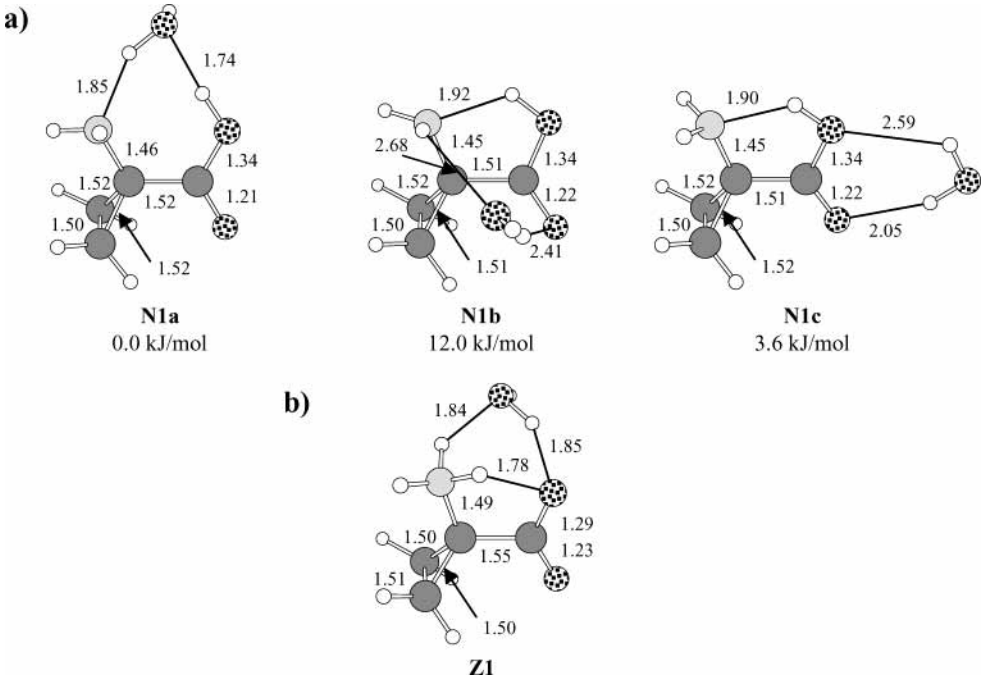

Figure 2. The **N** (a) and **Z** (b) structures of the ACC·H_2O cluster in the gas phase optimized at the B3LYP/6-31G(d) level. Bond lengths are shown in angstroms. The relative stabilities are shown in kJ/mol.

to that for isolated Gly.[47,48] This tendency, however, has been reversed, as shown in Figure 1a in aqueous solution. The optimized structure **N0c** including aqueous solution effect is favored over the others. These energetics were taken into account regardless the type of solvation model used. It is well known that the effect of the aqueous solvation alters the preference in this case of Gly.[22] The stabilization is controlled by a dipole moment of a solute, i.e., this is ascribed to the large dipole moment of 18.9×10^{-30} Cm for **N0c** vs 5.2×10^{-30} Cm for **N0b** and 4.0×10^{-30} Cm for **N0a**. It will seemingly be reasonable to consider the structure **N0c** as a stable **N** form of ACC in water. The geometry optimization of the **Z** form of ACC in the gas phase failed to converge as well as Gly. This occurred even when solvent effects were taken into account by using the Onsager model. Note that only the PCM calculation locates the **Z** form of ACC (**Z0**) as an energy minimum, which is 22.6 kJ/mol less stable than the **N0c** (Figure 1b). The results suggest the necessity of specific local interactions between water molecules and ACC to fully stabilize the **Z** form; thus, we repeated the calculations by including one or more water molecules in the simulation.

3.2. Model of Short-Range Local Interactions. We tried to coordinate a water molecule to various spaces around ACC and determine the optimized monohydrated ACC species. Figure 2a illustrates our obtained stable structures of **N** forms in the monohydrated ACC. We adapt the structure **N0c** as the stable form in water as mentioned in the previous section, so that we add one water molecule to **N0c** in the similar way for recent calculations on Gly.[18,19] The water molecule bridges the carbonyl and amine groups with two hydrogen bonds in **N1a** and **N1b** while it is doubly hydrogen bonded to the carboxyl group in **N1c**. In the calculation on Gly,[19] it is shown that the structure similar to **N1a** has the largest binding energy. In accordance with this result, **N1a** with the bridging water molecule is 4−12 kJ/mol more stable than the **N1c** and **N1b**. In **N1a**, the large binding energy is gained by the bridging water molecule, although the monohydration makes the NCCO moiety nonplaner (NCCO angle: 10.5°). Figure 2b shows the stable structure of the **Z** form of ACC optimized at the B3LYP/6-31G(d) level. Though we sought the **Z** forms that correspond to the three **N** forms, **N1a**, **N1b**, and **N1c**, the structure **Z1** originating from **N1a** was located on the minimum. The other optimizations of **Z** forms, which correspond to **N1b** and **N1c**, converge into the original neutral forms. In **Z1**, the water molecule bridges the carbonyl and amine groups so as to stabilize the positive and negative charges of NH_3^+ and COO^- ions, though the structure is 48.1 kJ/mol less stable than the **N1a**. These results suggest that the bridging water molecule is of importance to stabilize both the **N** and **Z** forms of ACC. We, therefore, will systematically construct the initial geometries for the larger cluster, ACC·$(H_2O)_n$, in a way that a water molecule is successively added to **Z1** so that the water molecule forms as many hydrogen bonds as possible. Then, only the corresponding **N** forms would be considered in order to gain the preliminary insight into the **N**-to-**Z** transition mechanism.

Figure 3 shows the optimized geometries of the most stable **Z** and **N** forms of the ACC·$(H_2O)_n$ ($n = 1-8$) clusters at the B3LYP/6-31G(d) level. For $n = 1$ and 2, the water molecules (**W1** and **W2**) hydrate both the amino and carboxyl groups by bridging them. As the cluster size increases from $n = 3-5$, water molecules (**W3**, **W4**, and **W5**) hydrate one of these two groups. For $n \geq 6$, some of the water molecules (such as **W6**) do not directly interact with either of the two functional groups but take part in water−water interactions so as to grow the hydrogen-bond network.

To determine the smallest adequate cluster model for the **N**-to-**Z** transition, we examined in detail the changes in ACC geometry as a function of cluster size. The N−C−C−O dihedral angle changed to values in the range 5−30° with increasing cluster size, suggesting the flexibility of the backbone moiety. The separation between N and O in the **N** form (ca. 2.85 Å) was almost consistent regardless of the cluster size. Although the separation between N and O in the **Z** form changed drastically on going from $n = 1$ to $n = 2$, it changed only slightly beyond $n = 3$. In examining the geometrical changes around the **W1** water, we can see a marked difference between the **N** and **Z** forms. As Figure 3 shows, the $r(O^{W1}-N)$ and $r(O-O^{W1})$ distances become shorter in the **N** form with

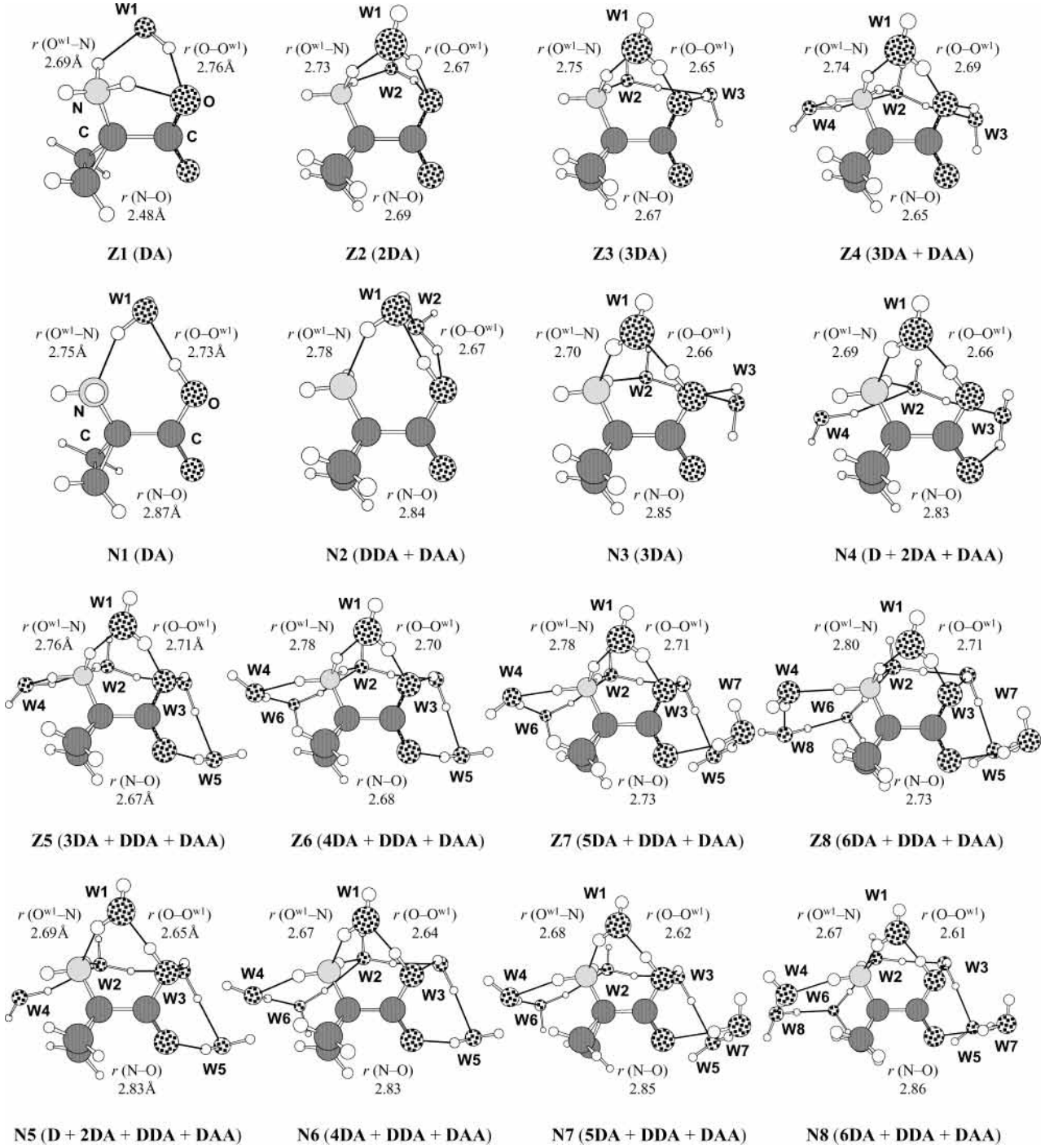

Figure 3. The **Nn** and **Zn** structures of ACC·$(H_2O)_n$ ($n = 1-8$) clusters in the gas phase optimized at the B3LYP/6-31G(d) level. The letters, **D** and **A**, indicate donor and acceptor, respectively. Bond lengths are shown in angstroms.

increasing cluster size, but in **Z** they become longer. The shortening of the $r(O^{W1}-N)$ and $r(O-O^{W1})$ distances in the **N** form may be explained by a cooperative enhancement of the interaction owing to the growth of a hydrogen-bond network involving the amino and carboxyl groups. On the other hand, both the positive and negative charges on the amino and carboxyl groups in the **Z** form are well dispersed into the network so that the ionic interactions between the two functional groups and **W1** are weakened with the growth of the hydrogen-bond network. Nevertheless, the changes in both the **N** and **Z** forms appear to be stabilized at $n \geq 6$.

Finally, we analyzed the types of hydrated water molecules based on their donor−acceptor pattern, where **DA** (Figure 3) represents a water molecule acting simultaneously as a hydrogen-bond donor (**D**) and acceptor (**A**), for instance. Although there were discrepancies in the donor−acceptor pattern between the **N** and **Z** forms in the $n \leq 5$ clusters, the discrepancy disappeared in the $n \geq 6$ clusters. For example, at $n = 4$, four water molecules (3**DA** + **DAA**) are fully involved in the hydrogen-bond network in the **Z** form. However, the presence of one **D** water (**W4**) in the **N** form makes the net stabilization less compared to the **Z** form. To consistently model local interactions in the **N** and **Z** forms, such loss in stabilization should be discarded.

Table 1 summarizes the stabilization energies of each **N** and **Z** form of the ACC·$(H_2O)_n$ ($n = 1-8$) clusters relative to that of the next-smaller cluster. The stabilization by added water is always greater for the **Z** form than for the **N**, owing to the ionic

TABLE 1: Stabilization Energies (in kJ mol^{-1}) for the N (ΔE^N) and Z (ΔE^Z) Forms of ACC·$(H_2O)_n$ ($n = 1-8$) Clusters in the Gas Phase, Calculated at the B3LYP/6-31G(d) Level[a]

	ACC·$(H_2O)_{n-1}$ + $H_2O \rightarrow$ ACC·$(H_2O)_n$			ACC^N·$(H_2O)_n \rightleftarrows$ ACC^Z·$(H_2O)_n$
n	δE^N	δE^Z	$\delta E^Z - \delta E^N$	ΔE
1	35.0	*b*	*b*	−48.1
2	49.5	80.2	30.7	−17.5
3	58.9	75.8	16.9	−0.6
4	43.5	54.3	10.8	10.3
5	66.3	80.1	13.8	24.0
6	66.2	75.8	9.6	33.7
7	57.8	65.1	7.3	41.0
8	57.6	61.4	3.8	44.8

[a] The relative stabilities of each **Z** form with respect to the corresponding **N** form, $\delta(E^Z - E^N)$, are also listed. [b] The values are not calculated, because the geometry optimization of the **Z** form without water molecules failed to converge.

nature of the interaction in the former. The stabilization due to the growth of the water−water network dominates the stabilization of the **N** and **Z** forms of the $n \geq 6$ clusters. We also show the relative energies of each **Z** form with respect to the corresponding **N** form, ΔE, in Table 1. The **Z** form is less stable in the clusters with $n = 1$ and 2. The **Z** form has stability comparable to the **N** form at $n = 3$, where the charge on the COO^- moiety in the **Z** form is well dispersed by hydration with **W1** and **W3**. In the $n \geq 4$ clusters, the **Z** form is energetically favored over the **N** form. The energy difference, ΔE, between the **Z** and **N** forms appears to converge to ~40 kJ mol^{-1} with increasing cluster size. Note that the inclusion of entropic effect leads to a rather small energy difference between the **Z** and **N** forms. For instance, the energy difference, ΔE, at $n = 6$ is 33.7 kJ mol^{-1}, while ΔG is 22.6 kJ mol^{-1}. Summarizing these results, the $n = 6$ cluster would be the smallest adequate model for short-range local ACC−water interactions.

TABLE 2: Relative Stability (in kJ mol^{-1}) without (ΔE) and with (ΔE^{ZPVC}) Zero-Point Vibrational Corrections of the Z Form with Respect to the N Form of the ACC·$(H_2O)_6$ Cluster in Both Gas and Solution Phases, Calculated at the B3LYP/6-31G(d) Level[a]

	gas phase	solution phase	change by solvation
ΔE	33.7	46.2	12.5
ΔE^{ZPVC}	27.3	42.4	15.1
ΔG	22.6	41.5	18.9

[a] The corresponding values of the free energy (ΔG) are also shown. The solvent effect was taken into account by using the Onsager model.

3.3. Effects of Long-Range Solvent Environment. The long-range effects of the water medium were simulated by using the Onsager model. The dipole moments of the **N** and **Z** forms of the ACC·$(H_2O)_6$ cluster were 8.0×10^{-30} and 18.7×10^{-30} Cm, respectively in the gas phase. This indicates that the **Z** form should show stronger interaction with a dielectric continuum than the **N** form. The optimized geometries of the **N** and **Z** forms of the ACC·$(H_2O)_6$ cluster calculated with the Onsager model did not significantly differ from those obtained without the Onsager model at the B3LYP/6-31G(d) level. Table 2 shows the relative stability of the **Z** form with respect to the **N** form of the $n = 6$ cluster. The long-range solvent effect stabilizes the **Z** form more than the **N** form, resulting in a higher energy difference ($\Delta E = 46.2$ kJ mol^{-1}) in the solvent than in the gas phase (33.7 kJ mol^{-1}) calculation. The zero-point vibrational correction does not significantly change the tendency. The effect of entropy reduces the energy difference (ΔG) in the gas phase, but the effect is almost negligible in the solution phase. Finally, to evaluate the energy difference between the **Z** and **N** forms as accurately as possible, we performed the optimization at the B3LYP/6-31+G(d,p) level with the Onsager model. The optimized geometries are not much different from those at the B3LYP/6-31G(d) level. The single-point PCM calculations were also performed at the geometries optimized

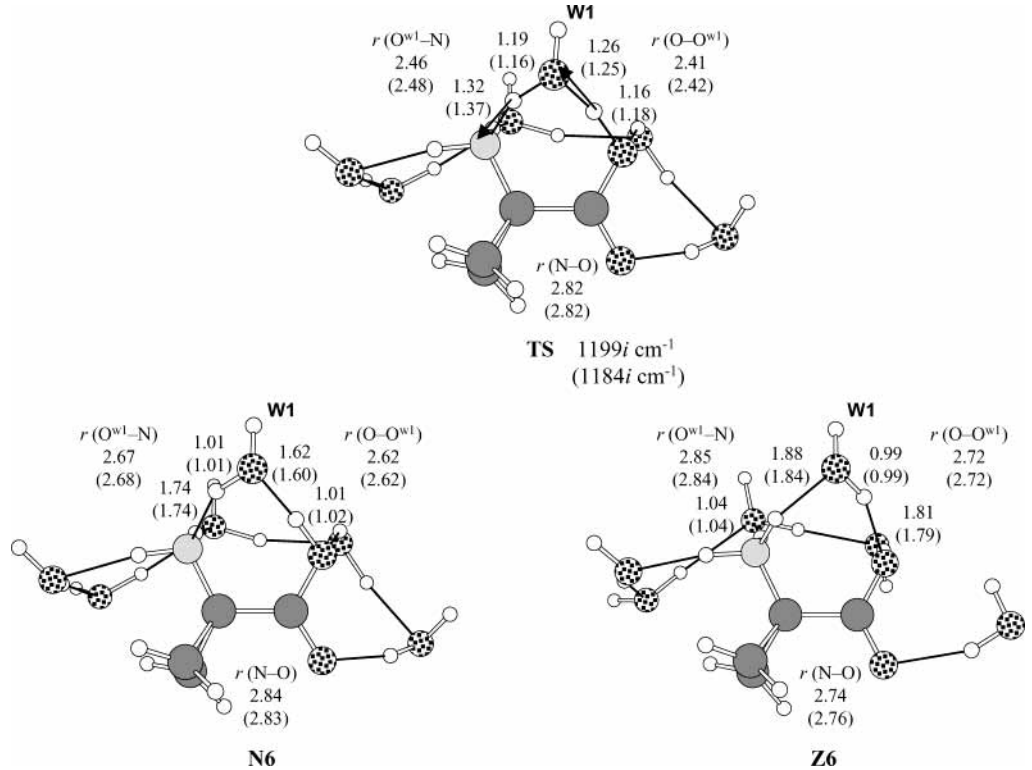

Figure 4. The **N**, transition-state (**TS**), and **Z** forms of ACC·$(H_2O)_6$ clusters calculated for the water-assisted mechanism at the B3LYP/6-31+G(d,p) level with the Onsager model. Bond lengths are shown in angstroms. The numbers in parentheses are those obtained at the B3LYP/6-31G(d) level.

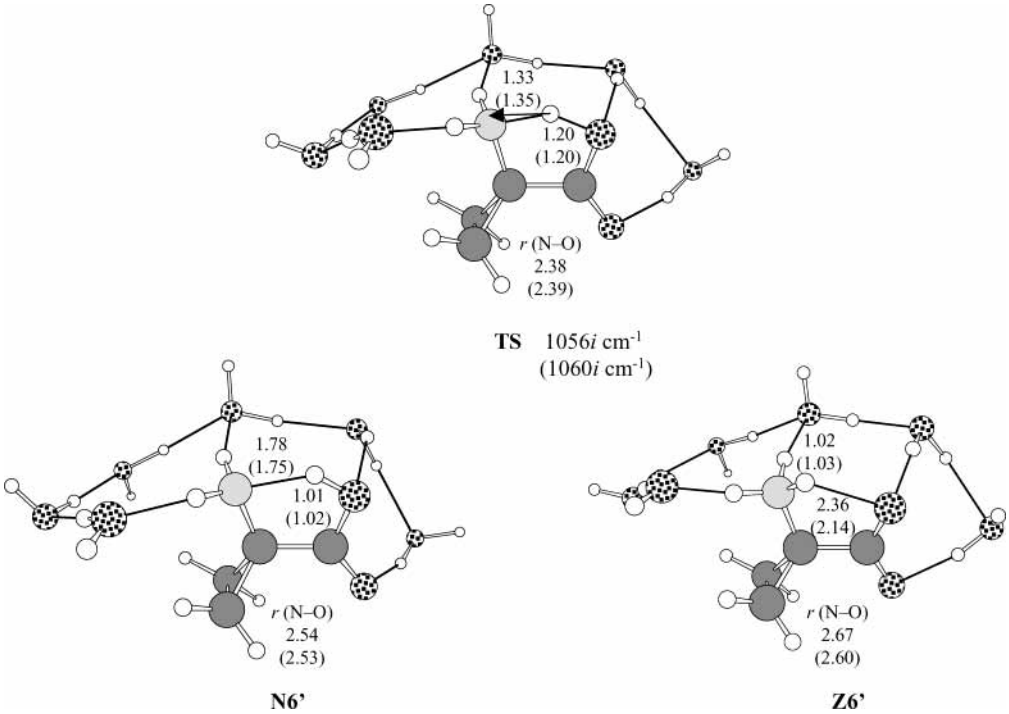

Figure 5. The **N**, **TS**, and **Z** forms of ACC·$(H_2O)_6$ clusters calculated for the direct mechanism at the B3LYP/6-31+G(d,p) level with the Onsager model. Bond lengths are shown in angstroms. The numbers in parentheses are those obtained at the B3LYP/6-31G(d) level.

TABLE 3: Relative Energies (in kJ mol^{-1}) without (ΔE) and with (ΔE^{ZPVC}) Zero-Point Vibrational Corrections, Calculated for the Structures of the ACC·$(H_2O)_6$ Cluster Occurring during Ionization, According to the Direct and Water-Assisted Proton-Transfer Reaction Mechanisms[a]

		water-assisted mechanism			direct mechanism		
		HF[b]	B3LYP[c]		HF	B3LYP[c]	
	structure	6-31G(d)	6-31G(d)	6-31+G(d,p)	6-31G(d)	6-31G(d)	6-31+G(d,p)
ΔE	**N**	0.0 (0.0)	0.0	0.0	0.0	0.0	0.0
	TS	73.6 (76.6)	13.4	15.1	43.9	9.2	10.5
	Z	−42.3 (−37.7)	−46.4	−46.4	−21.8	−33.1	−39.5
ΔE^{ZPVC}	**N**	0.0 (0.0)	0.0	0.0	0.0	0.0	0.0
	TS	60.7 (65.3)	0.8	2.4	35.1	2.1	2.5
	Z	−33.5 (−29.7)	−42.3	−42.9	−13.0	−25.9	−35.3
ΔG	**N**	0.0 (0.0)	0.0	0.0 (0.0)	0.0	0.0	0.0 (0.0)
	TS	71.1	5.9	9.4 (16.9)	40.6	0.4	5.1 (14.5)
	Z	−28.0 (−20.9)	−41.4	−42.2 (−42.3)	−4.6	−25.5	−32.0 (−39.2)

[a] Calculations were performed at the HF/6-31G(d), B3LYP/6-31G(d), and B3LYP/6-31+G(d,p) levels with both the Onsager model and PCM. The corresponding free energy values (ΔG) are also shown. [b] The numbers in parentheses are the corresponding values for the hydrated cluster of glycine, Gly·$(H_2O)_6$, taken from ref 24. [c] The numbers in parentheses were obtained by the single-point PCM calculations at the optimized geometries with the Onsager model.

by the B3LYP/6-31+G(d,p) method. Our best estimate using the PCM for the free-energy difference between the **N** and **Z** forms of ACC in solution is 42.3 kJ mol^{-1}, which corresponds to an equilibrium constant of 2.6×10^7. This value is very close to that experimentally reported for the Gly (2.4×10^5) by Wada et al.[49]

3.4. Water-Assisted Proton Transfer. Two mechanisms have been proposed for the **N**-to-**Z** transition: direct proton transfer and water-assisted proton transfer. Figure 4 shows the optimized geometries of the reactant (**N**), transition-state (**TS**), and product (**Z**) species of ACC according to the water-assisted proton-transfer mechanism, calculated at the B3LYP/6-31G(d) and 6-31+G(d,p) levels with the Onsager model. These two methods give very similar geometries for **N**, **TS**, and **Z** species. We found a single **TS** for the water-assisted mechanism, indicating that the two protons move in a concerted fashion via a "water bridge" (**W1**). In the **TS**, the $r(O^{W1}-N)$ and $r(O-O^{W1})$ distances are equally shortened by 0.2 Å, compared to those in the reactant (**N**), although the separation between N and O is nearly the same in the **N** and **TS** forms. The calculated imaginary frequency is 1199*i* cm^{-1} at the B3LYP/6-31+G(d,p) level. In the product (**Z**), the $r(O^{W1}-N)$ and $r(O-O^{W1})$ distances returned to longer values, but ionic interaction between the NH_3^+ and COO^- moieties makes the distance between N and O in **Z** about 0.1 Å shorter than in **N**.

The corresponding geometries for the direct mechanism are shown in Figure 5. The separations between N and O were all 0.2−0.4 Å shorter than those calculated for the water-assisted mechanism. In going from the **N** to **T**, the separation between N and O became 0.1 Å shorter, although this distance did not strikingly change in the water-assisted mechanism. At the B3LYP/6-31+G(d,p) level, the imaginary frequency is 1056*i* cm^{-1}, indicating the relatively slow motion of the proton in the direct mechanism. The **Z** product is slightly less stable than the **Z** product in the water-assisted mechanism.

Table 3 summarizes the energetics of the direct and water-assisted proton-transfer reaction mechanisms, as calculated at the HF/6-31G(d), B3LYP/6-31G(d) and B3LYP/6-31+G(d,p)

levels. At the B3LYP/6-31+G(d,p) level, the calculated exothermicity without (ΔE) and with (ΔE^{ZPVC}) zero-point vibrational corrections are 6.9 and 7.6 kJ mol^{-1}, respectively, larger for the water-assisted mechanism than for the direct mechanism. The corresponding calculated value of free energy at room temperature was 10.2 kJ mol^{-1}. The barrier height (ΔE) for the water-assisted mechanism was 15.1 kJ mol^{-1}, which is 4.6 kJ mol^{-1} higher than that for the direct mechanism at the B3LYP/6-31+G(d,p) level, although the zero-point vibrational correction yielded comparable barrier heights for both mechanisms. We obtained an energy barrier ($\Delta G^{\ddagger}$) of 9.4 kJ mol^{-1} for the water-assisted mechanism, which is only 4.3 kJ mol^{-1} higher than that for the direct mechanism. The barrier height refined by the single-point PCM calculations does not change the propensity; that is, $\Delta G^{\ddagger} = 16.9$ kJ mol^{-1} for the water-assisted mechanism, which is 2.4 kJ mol^{-1} higher than that for the direct one.

Although the calculated barrier height may be an underestimation, because the B3LYP method tends to estimate barrier heights lower,[40] the HF results indicate that the qualitative picture could be preserved. As Table 3 shows, our results for the ACC·$(H_2O)_6$ cluster agree well with those obtained for the hydrated cluster of glycine, Gly·$(H_2O)_6$ by Fernández-Ramos et al.[24] The exothermicity at the HF/6-31G(d) level is slightly higher for ACC·$(H_2O)_6$ than for Gly·$(H_2O)_6$. Accordingly, the barrier height is ~5 kJ mol^{-1} lower for ACC·$(H_2O)_6$.

Consequently, it is possible for first-neighbor water molecules to assist or even directly participate in the reaction, even though the water-assisted mechanism is slightly less energetically favorable than the direct mechanism.

4. Conclusions

The proton-transfer mechanism for ionization of the hydrated cluster of ACC, which is a crucial precursor in the ethylene biosynthetic pathway in plants, was investigated theoretically to determine to what extent water molecules may contribute to the mechanism of synthesis. Short-range local ACC−water interactions were satisfactorily modeled by a cluster of ACC with 6 water molecules. The long-range effects of water media were accounted for by both the Onsager model and PCM. We have reasonably predicted that the free-energy difference between the neutral and zwitterionic forms of the ACC·$(H_2O)_6$ cluster is 42.3 kJ mol^{-1}. We have shown that the neutral-to-zwitterion transition proceeds by either the direct or water-assisted proton-transfer mechanism with an energy barrier ($\Delta G^{\ddagger}$) of, at most, 16.9 kJ mol^{-1}. The neighboring water molecules directly participate in the ionization process, indicating that water molecules should significantly contribute to the reaction that forms ethylene from the ACC precursor. This work demonstrates that a combined calculation approach using both the discrete and dielectric continuum models is such an efficient tool that it should shed light on molecular aspects of plant biology.

References and Notes

(1) Ben-Nun, M.; Martínez, T. J. *Chem. Phys.* **2000**, *259*, 237.
(2) Neljubow, D. *Bot. Zentralbl.* **1901**, *10*, 128.
(3) Adams, D. O.; Yang, S. F. *Proc. Natl. Acad. Sci. U. S. A.* **1979**, *76*, 170−174.
(4) Yang, S. F.; Hoffman, N. E. *Annu. Rev. Plant Physiol.* **1984**, *35*, 155.
(5) Fluhr, R.; Mattoo, A. K. *Crit. Rev. Plant Sci.* **1996**, *15*, 479.
(6) John, P. *Physiol. Plant.* **1997**, *100*, 583.
(7) Hamilton, A. J.; Lyett, G. W.; Grierson, D. *Nature* **1990**, *346*, 284.
(8) Hamilton, A. J.; Bouzayen, M.; Grierson, D. *Proc. Natl. Acad. Sci. U. S. A.* **1991**, *88*, 7434.
(9) Ververidis, P.; John, P. *Phytochemistry*, **1991**, *30*, 725.
(10) Dong, I. G.; Fernández-Maculet, J. C.; Yang, S. F. *Proc. Natl. Acad. Sci. U. S. A.* **1992**, *89*, 9789.
(11) Rocklin, A. M.; Tierney, D. L.; Kofman, V.; Brunhuber, N. M. W.; Hoffman, B. M.; Christoffersen, R. E.; Reich, N. O.; Lipscomb, J. D.; Que, L., Jr. *Proc. Natl. Acad. Sci. U. S. A.* **1999**, *96*, 7905.
(12) Zhou, J.; Rocklin, A. M.; Lipscomb, J. D.; Que, L., Jr.; Solomon, E. I. *J. Am. Chem. Soc.* **2002**, *124*, 4602.
(13) Yang, S. F.; Dong, J. G. *Bot. Bull. Acad. Sin.* **1993**, *34*, 89.
(14) Bonaccorsi, R.; Palla, P.; Tomasi, J. *J. Am. Chem. Soc.* **1984**, *106*, 1945.
(15) Truong, T. N.; Stefanovich, E. V. *J. Chem. Phys.* **1995**, *103*, 3709.
(16) Andzelm, J.; Kolmel, C.; Klamt, A. *J. Chem. Phys.* **1995**, *103*, 9312.
(17) Tortonda, F. R.; Pascual-Ahuir, J. L.; Silla, E.; Tuñón, I.; Ramírez, F. J. *J. Chem. Phys.* **1998**, *109*, 592.
(18) Tortonda, F. R.; Pascual-Ahuir, J. L.; Silla, E.; Tuñón, I.; Ramírez, F. J. *THEOCHEM* **2003**, *623*, 203.
(19) Basch, H.; Stevens, W. J. *Chem. Phys. Lett.* **1990**, *169*, 275.
(20) Jensen, J. H.; Gordon, M. S. *J. Am. Chem. Soc.* **1995**, *117*, 8159.
(21) Ding, Y.; Krogh-Jespersen, K. *J. Comput. Chem.* **1996**, *17*, 338.
(22) Tortonda, F. R.; Pascual-Ahuir, J. L.; Silla, E.; Tunñón, I. *Chem. Phys. Lett.* **1996**, *260*, 21.
(23) Kassab, E.; Langlet, J.; Evleth, E.; Akacem, Y. *THEOCHEM* **2000**, *531*, 267.
(24) Fernández-Ramos, A.; Smedarchina, Z.; Siebrand, W.; Zgierski, M. Z. *J. Chem. Phys.* **2000**, *113*, 9714.
(25) Bandyopadhyay, P.; Gordon, M. S.; Mennucci, B.; Tomasi, J. *J. Chem. Phys.* **2002**, *116*, 5023.
(26) Shoeib, T.; Ruggiero, G. D.; Siu, K. W. M.; Hopkinson, A. C.; Williams, I. H. *J. Chem. Phys.* **2002**, *117*, 2762.
(27) Cui, Q. *J. Chem. Phys.* **2002**, *117*, 4720.
(28) Torrent, M.; Mogi, K.; Basch, H.; Musaev, D. G.; Morokuma, K. *J. Phys. Chem. B* **2001**, *105*, 8616.
(29) Senn, H. M.; Margl, P. M.; Schmid, R.; Ziegler, T.; Blöchl, P. E. *J. Chem. Phys.* **2003**, *118*, 1089.
(30) Topol, I. A.; Burt, S. K.; Rashin, A. A. *Chem. Phys. Lett.* **1995**, *247*, 112.
(31) Novoa, J. J.; Soza, C. *J. Chem. Phys.* **1995**, *99*, 15837.
(32) Soliva, R.; Orozco, M.; Luque, F. J. *J. Comput. Chem.* **1997**, *18*, 980.
(33) Gonzalez, L.; Mo, O.; Yanez, M. *J. Comput. Chem.* **1997**, *18*, 1124.
(34) Jiang, J. C.; Tsai, M.-H. *J. Phys. Chem. A* **1997**, *101*, 1982.
(35) Sirois, S.; Proynov, E. I.; Nguyen, D. T.; Salahub, D. R. *J. Chem. Phys.* **1997**, *107*, 6770.
(36) Tortonda, F. R.; Pascual-Ahuir, J. L.; Silla, E.; Tuñón, I.; Ramírez, F. J. *J. Chem. Phys.* **1998**, *109*, 592.
(37) Re, S.; Osamura, Y. *J. Phys. Chem. A* **1998**, *102*, 3798.
(38) Re, S.; Osamura, Y.; Suzuki, Y.; Schaefer, H. F. *J. Chem. Phys.* **1998**, *109*, 973.
(39) Re, S.; Osamura, Y.; Morokuma, K. *J. Phys. Chem. A* **1999**, *103*, 3535.
(40) Sadhukhan, S.; Muñoz, D.; Adamo, C.; Scuseria, G. E. *Chem. Phys. Lett.* **1999**, *306*, 83.
(41) Lee, C.; Yang, W.; Parr, R. G. *Phys. Rev. B* **1988**, *37*, 785.
(42) Becke, A. D. *J. Chem. Phys.* **1993**, *98*, 1372.
(43) Onsager, L. *J. Am. Chem. Soc.* **1936**, *58*, 1486.
(44) Miertus, S.; Scrocco, E.; Tomasi, J. *Chem. Phys.* **1981**, *55*, 117.
(45) Hall, N. E.; Smith, B. J. *J. Phys. Chem. A.* **1998**, *102*, 3985.
(46) Frisch, M. J.; Trucks, G. W.; Schlegel, H. B.; Scuseria, G. E.; Robb, M. A.; Cheeseman, J. R.; Zakrzewski, V. G.; Montgomery, J. A., Jr.; Stratmann, R. E.; Burant, J. C.; Dapprich, S.; Millam, J. M.; Daniels, A. D.; Kudin, K. N.; Strain, M. C.; Farkas, O.; Tomasi, J.; Barone, V.; Cossi, M.; Cammi, R.; Mennucci, B.; Pomelli, C.; Adamo, C.; Clifford, S.; Ochterski, J.; Petersson, G. A.; Ayala, P. Y.; Cui, Q.; Morokuma, K.; Malick, D. K.; Rabuck, A. D.; Raghavachari, K.; Foresman, J. B.; Cioslowski, J.; Ortiz, J. V.; Stefanov, B. B.; Liu, G.; Liashenko, A.; Piskorz, P.; Komaromi, I.; Gomperts, R.; Martin, R. L.; Fox, D. J.; Keith, T.; Al-Laham, M. A.; Peng, C. Y.; Nanayakkara, A.; Gonzalez, C.; Challacombe, M.; Gill, P. M. W.; Johnson, B. G.; Chen, W.; Wong, M. W.; Andres, J. L.; Head-Gordon, M.; Replogle, E. S.; Pople, J. A. Gaussian 98, revision A.7; Gaussian, Inc.: Pittsburgh, PA, 1998.
(47) Jensen, J. H.; Gordon, M. S. *J. Am. Chem. Soc.* **1991**, *113*, 7917.
(48) Hu, C.-H.; Shen, M.; Schaefer, H. F. *J. Am. Chem. Soc.* **1993**, *115*, 5, 2923.
(49) Wada, G.; Tamura, E.; Okina, M.; Nakamura, M. *Bull. Chem. Soc. Jpn.* **1982**, *55*, 3064.